

## Topology Optimization of Cellular Materials for Properties Governed by Nonlinear Mechanics

Josephine V. Carstensen<sup>1</sup>, Reza Lotfi<sup>1</sup>, James K. Guest<sup>1</sup>

<sup>1</sup> Civil Engineering Department, Johns Hopkins University, Maryland, USA, jvcarstensen@jhu.edu, reza.lotfi@gmail.com and jkguest@jhu.edu

### 1. Abstract

Topology optimization offers a means to leverage the advancement in manufacturing technologies that in recent years have made it possible to fabricate cellular materials with complex but prescribed topologies. Topology optimization has previously been used for unit cell design of materials with elastic properties and herein we look to extend these approaches to design materials with properties that are governed by nonlinear mechanics, such as energy absorption. One of the primary challenges in this setting is the lack of unit cell upscaling techniques for nonlinear behaviour, including both material and geometric nonlinearities. In its absence, we turn instead to the assumption of finite periodicity. The proposed formulation uses existing nonlinear sensitivity analysis schemes as the backbone of the design algorithm. Two new topologies optimized for energy absorption are presented and experimental results of actual fabricated samples are discussed.

**2. Keywords:** Topology optimization, nonlinear mechanics, cellular materials.

### 3. Introduction

In recent years manufacturing techniques and controls have improved significantly, making it possible to fabricate cellular materials with increasingly complex topologies. Cellular materials herein refers to materials that are periodic and porous. This technological advancement makes two questions relevant: (1) how does the topology influence the bulk material properties (the forward problem); and (2) what is the unit cell topology that optimizes these effective properties? (the inverse problem). The focus of this work is to use topology optimization to solve the inverse problem and hence to design cellular materials with optimized effective properties. Specifically we seek to design an effective material of Bulk Metallic Glass with a maximized energy absorption. This is a nonlinear property and will therefore require both geometric and material nonlinearities to be included in the problem formulation.

Several researchers have used topology optimization to design materials with optimized effective (homogenized) properties, including elastic properties such as negative Poisson's ratio [1], thermoelastic [2], fluid permeability [3, 4], and stiffness- thermal conductivity [5]. These works, however, all consider linear properties, enabling analysis (and design) of a single unit cell to estimate effective bulk properties through homogenization.

In this paper we will discuss elastic cellular material design and how the design problem changes when designing for nonlinear mechanical properties. This is all done using a density based topology optimization approach with the well-known SIMP [6, 7] penalization scheme to give preference to 0-1 solutions and the Method of Moving Asymptotes [8] as the gradient-based optimizer.

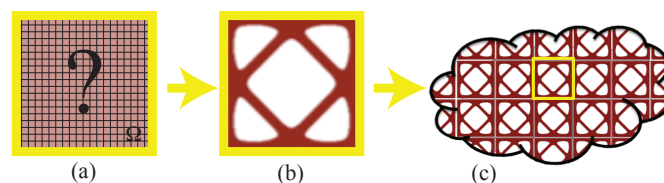


Figure 1: (a) discretized unit cell, (b) optimized unit cell topology and (c) unit cells in cellular material.

### 4. Design of Cellular Materials with Elastic Properties

Topology optimization for design of cellular materials can be illustrated by the schematic in Fig. 1, where Fig. 1a shows how the characteristic unit cell is defined as the design domain  $\Omega$ . The problem is posed formally as an optimization problem whose solution gives the optimized unit cell topology, as seen in Fig. 1b. Finally, Fig. 1c illustrates the periodic arrangement of the unit cell to form a cellular material, and underscores the need to estimate

effective material properties from analysis of the unit cell structure. When designing for linear elastic properties, the topology optimization problem is often posed as:

$$\begin{aligned}
& \underset{\phi}{\text{minimize}} && f(\phi, \mathbf{C}^H) \\
& \text{subject to} && \mathbf{K}(\phi) \mathbf{d}^{(i)} = \mathbf{f}^{(i)} \quad \forall i \\
& && g(\mathbf{C}^H(\phi, \mathbf{d}^{(i)})) \geq g_{min} \\
& && V_{min} \leq \sum_{e \in \Omega} \rho^e(\phi) v^e \leq V_{max} \\
& && \phi_{min} \leq \phi_n \leq \phi_{max} \quad \forall n \in \Omega \\
& && \mathbf{d}^{(i)} \text{ is } \Omega\text{-periodic}
\end{aligned} \tag{1}$$

Here  $f$  is the objective function that can be chosen as some (negative if maximizing) effective property such as Young's-, shear or bulk modulus or Poisson's ratio. Further,  $\phi$  is the design variables and stress and strain are denoted by  $\sigma$  and  $\varepsilon$  under the small strain assumption.  $\mathbf{K}(\phi)$  is the global stiffness matrix and constraints are defined by  $g$  with allowable magnitude  $g_{min}$ . A typical constraint, for example, is elastic symmetry, which is usually chosen as either square symmetric or isotropic. The bounds on the volume fraction or relative density are defined by  $V_{min}$  and  $V_{max}$  and  $\phi_{max}$  and  $\phi_{min}$  describes the design variable bounds that in this work are taken as 0 and 1. The element volume is denoted  $v^e$  and  $\rho^e(\phi)$  is the element density of element  $e$ .  $\mathbf{C}^H$  is the homogenized constitutive matrix computed using numerical homogenization and hence by applying test strain fields  $\varepsilon^{0(i)}$  to the unit cell. In Eq.(1),  $\mathbf{d}^{(i)}$  and  $\mathbf{f}^{(i)}$  are the displacements and force vectors for the test strain field  $i$ . The homogenization follows the description in [9]:

$$\mathbf{C}_{ij}^H = \frac{1}{|\Omega|} \sum_{e \in \Omega} (\mathbf{d}_0^{e(i)} - \mathbf{d}^{e(i)})^T \mathbf{K}^e(\phi) (\mathbf{d}_0^{e(j)} - \mathbf{d}^{e(j)}) \tag{2}$$

Here  $\mathbf{d}_0^{e(i)}$  is the vector of nodal displacements for element  $e$  corresponding to the test strain field  $\varepsilon^{0(i)}$  and  $\mathbf{K}^e(\phi)$  is the element stiffness matrix.

#### 4.1. Penalization of intermediate values

The element stiffnesses are related to the topology using the Solid Isotropic Material with Penalization (SIMP) method [6, 7] and the Young's modulus of the element therefore expressed as

$$E^e(\phi) = ((\rho^e)^\eta + \rho_{min}^e) E_0^e \tag{3}$$

where  $\eta \geq 1$  is the exponent penalty term,  $E_0^e$  is the Young's modulus of a pure solid element and  $\rho_{min}^e$  is a small positive number to maintain positive definiteness of the global stiffness matrix.

#### 4.2. Heaviside Projection Method

To improve the manufacturability of the topology-optimized designs we herein control the minimum length scale of the topological features. The length scale is generally defined as the minimum radius or diameter of the material phase of concern, here the solid phase. It is well established that controlling the length scale has the additional advantage that it circumvents numerical instabilities, such as checkerboard patterns and mesh dependency.

Several methods for controlling the length scale of a topology optimization design exist. Herein, the Heaviside Projection Method (HPM) [10] is used, since the operator of this method is capable of yielding 0-1 designs in which the minimum length scale is fulfilled without adding constraints to the problem. In HPM, the design variables are associated with a material phase and projected onto the finite elements by a Heaviside function. The problem is thus separated into two spaces; a design variable space, where the optimization is performed, and a finite element space, where the physical equilibrium is solved. The connection between the two spaces is the projection which typically is done radially. Therefore, the projection radius can easily be chosen as the prescribed minimum length scale  $r_{min}$ . Computationally a neighborhood  $N^e$  that records the design variables within the distance  $r_{min}$  is set up for each element. The design variables are mapped onto the elements by computing a weighted average  $\mu^e(\phi)$ , often called linear filtering, and to obtain binary solutions, the average design variables  $\mu^e(\phi)$  are passed through a Heaviside function to obtain the element volume fraction  $\rho^e$ .

$$\rho^e = 1 - e^{-\beta \mu^e(\phi)} + \frac{\mu^e(\phi)}{\phi_{max}} e^{-\beta \phi_{max}} \tag{4}$$

Here  $\beta \geq 0$  dictates the curvature of the regularization which approaches the Heaviside function as  $\beta$  approaches infinity. For full algorithmic details please see [10].

### 4.3. Sensitivities

The sensitivities of the objective function are calculated as follows:

$$\frac{\partial f}{\partial \phi_i} = \sum_{e \in \Omega} \frac{\partial f}{\partial \rho^e} \frac{\partial \rho^e}{\partial \phi_i} \quad (5)$$

The partial derivative of the objective function  $f$  with respect to the element volume fraction  $\rho^e$  is problem dependent and calculated using the adjoint method. The partial derivative of the element volume fraction with respect to the design variables follows the chain rule. By differentiating Eq.(4) the following expression is found:

$$\frac{\partial \rho^e}{\partial \phi_i} = \left( \beta e^{-\beta \mu^e(\phi)} + \frac{1}{\phi_{max}} e^{-\beta \phi_{max}} \right) \frac{\partial \mu^e}{\partial \phi_i} \quad (6)$$

## 5. Design of Cellular Materials with Nonlinear Properties

Topology optimization for energy absorption requires considering the fully nonlinear response of the designed structure. This thus includes material nonlinearities and geometric nonlinearities. In this research we optimize for both types of nonlinearities by combining the existing sensitivity formulations for material and geometric nonlinearities under displacement controlled loading from [13] and [12], respectively. This means that finite deformations are included and that we describe the nonlinear material behavior by Von Mises yield function with isotropic hardening. An elasto-plastic material model is used and we assume linear hardening. The SIMP approach is extended as in [12], however, we have used the same SIMP exponent for all the material parameters.

Topology optimization for nonlinear effective properties is a far more challenging task than for linear properties. Homogenization of nonlinear mechanics from unit cell analysis is not yet established, and thus we perform the optimization of a sample with finite periodicity. Effective elastic properties and symmetries are estimated using elastic homogenization as dictated by the problem formulation, leading to a unit cell topology optimization problem with analysis conducted over two different domains: the unit cell for elastic properties and structure with finite periodicity for the nonlinear properties. The problem formulation used herein is as follows:

$$\begin{aligned} & \underset{\phi}{\text{minimize}} && f(\phi, \mathbf{C}^H, \mathbf{S}, \mathbf{E}) \\ & \text{subject to} && \mathbf{K}_E(\phi) \mathbf{d}_E^{(i)} - \mathbf{f}_E^{(i)}(\phi) \quad \forall \quad i \\ & && \mathbf{R}^t(\phi, \mathbf{d}) = \mathbf{K}^t(\phi, \mathbf{d}) \mathbf{d}^t - \mathbf{f}^t(\phi) = 0 \quad \forall \quad t \\ & && g_E(\mathbf{C}^H(\phi, \mathbf{d}_E^{(i)})) \geq g_{E,min} \\ & && g_{NL}(\boldsymbol{\sigma}(\phi, \mathbf{d}), \boldsymbol{\varepsilon}(\phi, \mathbf{d})) \geq g_{NL,min} \\ & && V_{min} \leq \sum_{e \in \Omega} \rho^e(\phi) v^e \leq V_{max} \\ & && \phi_{min} \leq \phi_n \leq \phi_{max} \quad \forall \quad n \in \Omega \\ & && \mathbf{d}_E^{(i)} \text{ is } \Omega\text{-periodic} \end{aligned} \quad (7)$$

where the subscript  $E$  refers to the elastic and  $_{NL}$  to the nonlinear parts. The superscript  $t$  refers to the current load step and  $\mathbf{d}^t$  is hence the displacement vector at the current load step and  $\mathbf{d}$  the displacement vector unto  $t$ . The elastic unit cell equilibrium is given by the first constraint, and constraints  $g_E$  include the effective elastic property constraints such as the symmetry conditions. The nonlinear equilibrium constraints are given in the second set of constraints, and constraints  $g_{NL}$  comprise nonlinear property constraints as needed. In Eq.(7) the equilibrium condition is described in terms of  $\mathbf{R}(\phi, \mathbf{d})$  which is the residual force vector. This equilibrium condition must be solved using an iterative nonlinear FE solver. For the designs presented in the following we have taken total absorbed energy as given by as the objective:

$$f = - \int_{\Omega} \int \boldsymbol{\sigma}^T d\boldsymbol{\varepsilon} d\Omega \quad (8)$$

### 5.1. Solids-Only Modeling in the Physical Space

It is well established that the modelling of void elements required by the density based topology optimization approach introduces numerical instabilities such as excessive distortions under finite deformations. In addition

the elements of negligible volume fraction are quite detrimental to analysis as they maximize the system to be solved and thus computational expense. They are, however, needed in the optimization process for reintroduction of material as the design evolves. It can therefore be said that they are necessary for the design portion of the optimization process, not the analysis.

Different methods for circumventing these instabilities such as re-meshing [14], modified nonlinear convergence criteria [13], and stabilizing the stiffness matrix following Gaussian elimination [15] have been proposed. These methods require a threshold  $\rho_t$  to be set below which element stiffness is considered negligible. In this work, we simply introduce artificial boundary conditions to degrees of freedom that are surrounded completely by void elements. This is achieved by marking the nodes of elements whose stiffness is to be modeled ( $\rho^e > \rho_t$ ). Nodes that are unmarked receive a temporary boundary condition. Equation numbering and finite element assembly proceed in the standard manner, although it is noted the assembly routine need not check the equation numbers of void elements (including along the structural interface). This process is performed at each design iteration where the solids-topology changes.

It should be noted that the solids only finite element modeling makes the  $\rho_{min}$  parameter in Eq.(3) unnecessary. Herein we have therefore used  $\rho_{min} = 0$ .

## 6. Design of a Cellular Bulk Metallic Glass

The cellular material topology optimization design problem stated in Eq. (7) for maximizing the absorbed energy considering both geometric and material nonlinearities has been used to design a cellular bulk metallic glass material. Bulk metallic glasses (BMGs) are a class of amorphous structural materials with high strength and elasticity. However, they typically exhibit a brittle failure mode in bulk form. It is therefore desirable to design a cellular material that introduces ductility to BMG material systems.

We have considered a number of maximum volume fractions, and report on solutions found using  $V_{max} = 10\%$  and  $V_{max} = 12.5\%$  herein. An elasto-plastic uniaxial behavior (based on a small strain formulation) is assumed for the solid phase and the following material properties are assumed:  $E = 86.9$  GPa,  $\nu = 0.375$ ,  $\sigma_{y0} = 1.475$  GPa and  $H_0 = 0.84$  GPa. Square symmetry conditions were applied and the minimum length scale of the topological features specified herein was  $1.2h$  where  $h$  is the side length of the finite element mesh. The results presented herein have  $h = 0.005$  mm.

As mentioned above, finite periodicity has been used in the lack of a recognized upscaling method for nonlinear mechanical properties. The finite sample is considered fixed horizontally and vertically at its bottom and at the top a downward displacement is applied vertically while horizontal movement is restricted. The presented unit cell designs were arrived at using a  $5 \times 5$  unit cell sample. The effect of the sample size on the response has been investigated and  $5 \times 5$  was found to have a reasonably converged response without an excessive computational effort.

The stopping criterion for the topology optimization problem is collapse initiation of a unit cell and contact is hence not considered.

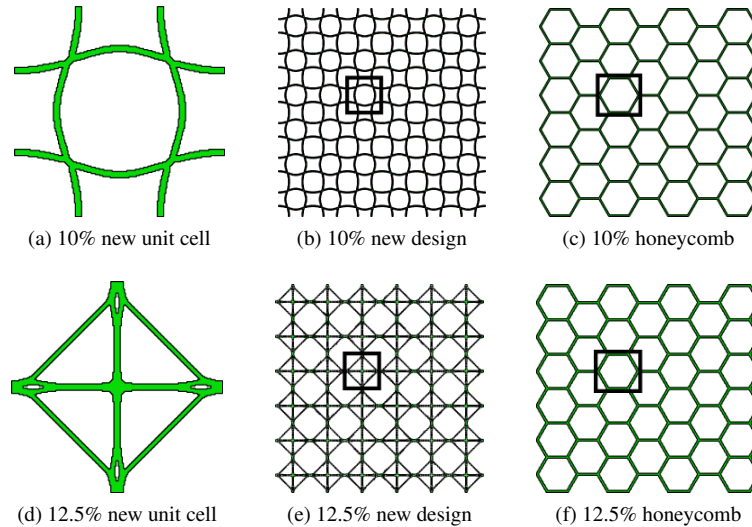


Figure 2: (a,d) unit cell and (b,e)  $6 \times 6$  periodic samples of cellular materials optimized for energy absorption. (c,f) are  $6 \times 6$  samples of honeycomb topologies.

In the proceeding, the numerical and experimental analyses are conducted on  $6 \times 6$  samples. The design solu-

tions are shown in Fig. 2 where both unit cells (a,e) and periodic samples of 6x6 unit cells (b,f) are given for the two considered volume fractions.

### 6.1. Numerical Analysis of the Stress-Strain Behavior

Samples of 6x6 unit cells are FE analyzed and compared to analyses of samples with the same volume fractions of  $V_{max} = 10\%$  and  $V_{max} = 12.5\%$ , respectively, and a more traditional honeycomb topology (Fig. 2c,f). Figure 3 contains the stress-strain responses of these analyses and the absorbed energies are indicated in the plots. We clearly see from the plots that the unit cell topology has a large effect on the response and absorbed energy of the effective bulk material. As expected, it is seen that the topology optimized designs has a higher level of energy absorption when measuring until instability that causes unit cell collapse is seen. These instabilities are found at different strains for all four considered samples. If comparing to the typical honeycomb topology the energy absorption is seen to be about 66% and 2% higher for the 10% and the 12.5% designs, respectively. It is interesting to note the difference in the deformation mechanisms used by two optimized the designs to achieve this improved energy absorbance. For the 10% volume fraction a soft material that can undergo large deformations before unit cell failure occurs is designed, whereas the 12.5% design has both higher strength and stiffness than the conventional honeycomb topology although this was not an objective of the optimization.

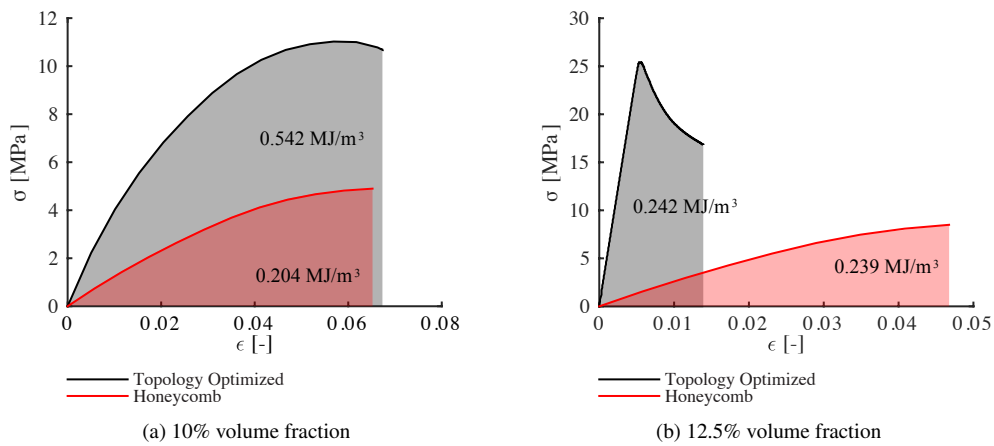


Figure 3: Stress-strain responses obtained from the FE-analyses of the considered sample topologies. The energy absorbed by each of the samples is indicated on the plot.

### 6.2. Experimental Results

A 6x6 unit cell sample of the designed topology with  $V_{max} = 12.5\%$  was fabricated in BMG and tested. A honeycomb sample with the same volume fraction was also fabricated and tested for comparison. The performed tests were uniaxial in-plane compression tests with quasi-static displacement control and the samples were tested till full densification. This is well beyond the stopping criterion of the optimization, but will enable the test to identify deformation mechanisms that would be beneficial to include in future optimization formulations.

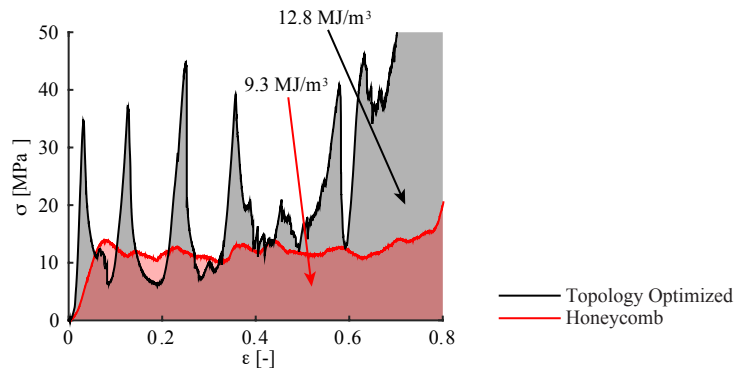


Figure 4: Stress-strain response from the experimental analysis of 6x6 samples with  $V_{max} = 12.5\%$ .

In the plot in Fig. 4 the experimental results are given and the amounts of energy absorbed by each of the two tested topologies are indicated. As expected, the energy absorption is significantly higher for the new de-

sign; an increase of about 38% is seen. This is higher than the improvement found by the numerical analysis, however a difference was expected as the two stopping criteria are not the same. Further, as in the numerical analysis the new design is seen to have a much higher initial stiffness and strength than the honeycomb topology. However, for both the honeycomb and the newly proposed topology the post initial peak behavior is seen to fluctuate and hence contain a series of peaks and drops. The amplitude of this cyclic behavior is most severe for the topology-optimized unit cell design. A future research focus is to alleviate this cyclic effect in the response.

## 7. Conclusion

The rapid improvement of manufacturing technologies presents a significant opportunity going forward in topology optimization for cellular material design. The design for elastic effective material properties is well understood, including optimization considering manufacturing constraints. Topology optimization-based design for nonlinear response properties of cellular material topologies, however, is significantly more challenging. As demonstrated, however, it also offers tremendous opportunities in designing materials with new capabilities.

## 8. Acknowledgements

Wen Chen and Jan Schroers from the Department of Mechanical Engineering and Material Science at Yale University, New Haven, Connecticut, are gratefully acknowledged for the experimental results in this paper. The work was supported by DARPA under the MCMA Program Award Number 60700-EG-DRP.

## 9. References

- [1] O. Sigmund, Materials with Prescribed Constitutive Parameters: An Inverse Homogenization Problem, *Struct. Multidisc. Optim.*, 31 (17), 2313-2329, 1994.
- [2] O. Sigmund and S. Torquato, Composites with extremal thermal expansion coefficients, *Applied Physics Letters*, 69 (21), 3203-3205, 1996.
- [3] J.K. Guest and J.H. Prévost, Design of maximum permeability material structures, *Int. J. Solids Structures*, 43 (22), 7028-7047, 2006.
- [4] V.J. Challis, J.K. Guest, J.F. Grotowski and A.P. Roberts, Computationally generated cross-property bounds for stiffness and fluid permeability using topology optimization, *Int. J. Solids Structures*, 49 (23), 3397-3408, 2012.
- [5] V.J. Challis, A.P. Roberts and A.H. Wilkins, Design of Three Dimensional Isotropic Microstructures for Maximized Stiffness and Conductivity, *Int. J. Solids Structures*, 45 (14), 4130-4146, 2008.
- [6] M.P. Bendsøe, Optimal shape design as a material distribution problem, *Structural Optimization*, 1 (4), 193-202, 1989.
- [7] G.I.N. Rozvany, M. Zhou and T. Birker, Generalized shape optimization without homogenization, *Structural Optimization*, 4 (3-4), 250-252, 1992.
- [8] K. Svanberg, The method of moving asymptotes: A new method for structural optimization, *Int. J. Numer. Meth. Engng.*, 24 (2), 359-373, 1987.
- [9] J. Guedes and N. Kikuchi, Preprocessing and postprocessing for materials based on the homogenization method with adaptive finite element methods, *Comput. Methods Appl. Mech. Engrg.*, 83 (2), 143-198, 1990.
- [10] J.K. Guest, J.H. Prévost and T. Belytschko, Achieving minimum length scale in topology optimization using nodal design variables and projection functions, *Int. J. Numer. Meth. Engng.*, 61 (2), 238-254, 2004.
- [11] T.E. Bruns and D.A. Tortorelli, Topology optimization of non-linear elastic structures and compliant mechanisms, *Comput. Methods Appl. Mech. Engrg.*, 190 (26), 3443-3459, 2001.
- [12] K. Maute, S. Schwarz and E. Ramm, Adaptive topology optimization of elastoplastic structures, *Structural Optimization*, 15 (2), 81-91, 1998.
- [13] T. Buhl, C.B.W. Pedersen and O. Sigmund, Stiffness design of geometrically nonlinear structures using topology optimization, *Struct. Multidisc. Optim.*, 19 (2), 93-104, 2000.
- [14] K. Maute and E. Ramm, Adaptive topology optimization, *Structural Optimization*, 10 (2), 100-112, 1995.
- [15] T.E. Bruns and D.A. Tortorelli, An element removal and reintroduction strategy for the topology optimization of structures and compliant mechanisms, *Int. J. Numer. Meth. Engng.*, 57 (10), 1413-1430, 2003.